IGSHPA Research Track
Las Vegas, December 6-8, 2022

Stationary and non-stationary deconvolution to recover long-term transfer functions

Gabriel Dion **Philippe Pasquier** **Denis Marcotte**
Gabrielle Beaudry

ABSTRACT

To design a ground heat exchanger, simulations are frequently used. One way to perform simulations is to use the well-known g-functions to obtain the ground temperature. These functions are usually obtained by analytical or numerical models, which limits the precision or takes long simulation time. Recent advances show that the short-term g-functions can also be retrieved by a deconvolution algorithm. However, the known deconvolution algorithm is only validated for a set of operating parameters and duration of less than 10 days. A first objective of this article is to demonstrate that longer g-functions can be retrieved with such an algorithm. Then, a second objective is to extend the application of the deconvolution to consider time varying operating parameters throughout a ground heat exchanger's operation. To achieve those objectives, the deconvolution will be first applied to various numerical year-long simulations of a ground source heat pump system with stationary conditions. Then, an extended multi-signal deconvolution will be applied to a non-stationary thermal response test of 30 days. Both tests show adequate temperature reconstruction with RMSE of less than 0.05 °C and 0.2 °C for the first and second scenarios respectively.

INTRODUCTION

Employing a geothermal heat pump connected to a ground heat exchanger (GHE) can significantly reduce a building's heating and cooling energy consumption, affecting positively the building sector's carbon emission (Omer, 2008; Sarbu & Sebarchievici, 2014). To design a GHE, simulations employing *g*-functions are commonly performed to compute the ground temperature (Eskilson, 1987). These functions describe the time evolution of the ground temperature along the borehole length to a unit impulse signal, and are generally used to find the borehole temperatures under a varying heating load (Zanchini & Lazzari, 2014). Various methods were developed to compute these functions. They rely on analytical (Cimmino & Bernier, 2013; Marcotte & Pasquier, 2014; Nguyen & Pasquier, 2021; Wei et al., 2016), polynomial (Zanchini & Lazzari, 2014), numerical (Robert & Gosselin, 2014) or block matrix (Dusseault et al., 2018) methodology. All these methods have limitations in some ways, either by assumption on analytical model or high computation cost to retrieve the site-specific *g*-function.

Recent advances have made it possible to use a deconvolution algorithm to obtain the short-term *g*-function (STgF) from the experimental data of a thermal response test (TRT) (Beier, 2020; Dion et al., 2022). Such an algorithm does not require a direct analytical or numerical model and directly uses the experimental data to obtain the STgF. Another advantage is that defining the STgF at the borehole outlet, as done by Dion et al. (2022), incorporates the thermal conductivity and capacity of the ground and of the GHE (e.g., casing, grout, pipe, and fluid). Such deconvolution

Gabriel Dion (gabriel.dion@polymtl.ca) is a Ph.D. candidate at Polytechnique Montréal, Canada.
Philippe Pasquier (philippe.pasquier@polymtl.ca) is professor of geological engineering at Polytechnique Montréal, Canada.
Denis Marcotte (denis.marcotte@polymtl.ca) is professor of geological engineering at Polytechnique Montréal, Canada.
Gabrielle Beaudry (gabrielle.beaudry@polymtl.ca) is a research associate at Polytechnique Montréal, Canada.

DOI: https://doi.org/10.22488/okstate.22.000019

algorithm performs an inversion on a set of nodes, so that the convolved temperatures are closest to their experimental counterparts. At publishing time, the deconvolution algorithm has not been used to obtain *g*-functions longer than periods or time representative of TRTs (e.g., 3 to 10 days).

Often, the heating power and the flow rate will vary to accommodate a heating demand, creating a system that is non-stationary through time. Recent advances in convolution algorithms allow to consider such non-stationary conditions and hands high quality results with both flow rate and heating power variations (Beaudry et al., 2021). To resolve such situations, several transfer functions are used (one for each state encountered) and convolved under the assumption of non-stationarity. Using such an approach, Beaudry et al., (2022) observed that including non-stationarity can ensure adequate ground temperatures and reduce peak demand to the electricity network.

On currently operating systems, temperatures at the inlet and outlet of a GHE are often available. However, matching these temperatures with a model is usually difficult because the input parameters used to design the GHE are often inaccurate, obtained with erroneous assumptions or do not consider heterogeneity. Therefore, using a calibrated model to evaluate the future response of a GHE under various operating parameters, analyze the performance and durability of a GHE or understanding a GHE's interaction with a nearby system is still a challenge. An alternative could be to use the experimental long-term *g*-function of a GHE and use it for simulations. Obtaining such experimental long-term *g*-function has never been done before.

The goals of this article are twofold: first to apply the single-deconvolution algorithm of Dion et al., (2022) to long GSHP system operation to obtain long-term *g*-function. Second, to provide an extension to the deconvolution algorithm of Dion et al. (2022) to recover a set of transfer functions corresponding to the different operating parameters in a GHE, occurring during the operation of a GSHP system.

METHODOLOGY

A deconvolution algorithm is simply the inverse of a convolution. Both convolution and deconvolution are usually only applied to stationary systems (e.g., a GHE with constant flow and bleed rates). It is, however, possible to consider non-stationarity, for which the specific case is stationarity. This section first presents the non-stationary convolution used for GSHP system and then, the deconvolution algorithm.

Non-Stationary Convolution (forward problem)

The forward model is based on the convolution equation, which is described with the equation:

$$T_{\mathrm{out}}(t) - T_0 = (f * g)(t) = \sum_{\mathrm{j}=1}^{\mathrm{i}} f(t_j) \cdot g(t_{i-\mathrm{j}+1}) \quad (1)$$

In this equation, f in is the excitation function and corresponds to the heating power change $f = Q(t_i) - Q(t_{i-1})$. T_0 is the initial ground temperature and T_{out} is the GHE borehole outlet temperature. The variable g is a transfer function, which corresponds to the variation of a system to a unit impulse. In the case of a GSHP system, it is the GHE response to an impulse of 1W throughout the length of the operation period. Hence, by normalizing f by 1W, the units of g are °C, which differs from the dimensionless *g*-function of Eskilson (1987). Hereinafter, the expression transfer function will be used to avoid misunderstanding but the underlying concept is the same.

Eq. (1) is valid for a steady circulation flow or bleed rate, which describes the state of the GHE operation. To account for state changes, during operation, Beaudry et al. (2021) incorporated a time dependence to the transfer function of Eq. (1), $g(t_{i-j+1}, t)$. In that way, the convolved borehole outlet temperature becomes a combination of the excitation function convolved by the corresponding transfer function. In that form, the combination results in discontinuous signal at the state changes. To correct the signal, a correction function is added to the convolution so that, for each state

transition, a corresponding state variation is applied. To the interested reader, the non-stationary convolution is described in greater details in Beaudry et al. (2021).

It is worth mentioning that the accuracy of the non-stationary convolution is within a mean-absolute-error of less than 0.06 °C on the operating temperature of a GSHP system. Hence, the method has a high accuracy, but is not an exact solution, as would be a stationary convolution.

Stationary or Non-Stationary Signal Deconvolution (inverse problem)

The deconvolution algorithm is akin to an optimization problem, in which the parameter to be optimized is the transfer function in Eq. (1). This section presents an extension to the algorithm of Dion et al., (2022) to deconvolve a set of transfer functions for the non-stationary case instead of a single one in a stationary scenario. The algorithm is closely related to the original one and can also be used for single-signal deconvolution.

Using a non-stationary convolution, multiple transfer functions can be obtained. To achieve that, a set of nodes τ_j (between 20 and 40 per function), spaced logarithmically on each transfer function, are selected as the optimization parameters. To reconcile the nodes τ_j and the time array t of the GSHP system operation, a piecewise cubic Hermite interpolation polynomial (PCHIP) is performed on each transfer function before the non-stationary convolution. The goal of the inversion is then to optimize the nodes values of each transfer function, so that the non-stationary convolution is close to the experimental operation temperatures $T = T_{out} - T_0$. The goal to attain is:

$$\hat{g}_{Set}(t) = arg\min_{\hat{g}(\tau_j)} \left(\left\| (\hat{T} - T_{Exp})(t) \right\|_2 \middle| C_1, C_2 \right) \tag{2}$$

In the previous equation, $\hat{g}_{set}$ is the estimated transfer functions obtained by deconvolution, τ_j are the nodes selected on each transfer function, t is the time vector, $\hat{T}$ is the estimated temperature obtained by non-stationary convolution, T_{Exp} is the experimental temperature. Finally, $\|\cdot\|_2$ is the l_2 norm.

In Eq. 2, the parameters C are positive derivative and negative second derivative constraints applied to each node of each transfer function. The first constraint is to impose the fact that the transfer function must be increasing with time. The second constraint reflects the general observation that the temperature is slowly reaching a steady state under a constant heating power. This is enforced by constraining the slope of the transfer function's first derivative to be strictly negative after a certain point. The two following equations describe the constraints, which are implemented in the optimization as linear inequality equations on the nodes.

$$C_1 \qquad 0 < \hat{\mathrm{g}}(\tau_j) < \hat{\mathrm{g}}(\tau_{j+1}) \; \forall \, j \in [0, n-1] \tag{3}$$

$$C_2 \qquad \hat{g}'(\tau_{j+1}) < \hat{g}'(\tau_j) \; \forall \, j \in [z, n-1] \tag{4}$$

where z is the node τ_j from which the first derivative has a negative slope.

To ensure faster convergence, a first approximation of the optimization problem is required. Here, an initial guess of the transfer function set used by the main optimization algorithm is obtained with the use of 2 subsequent inversion problems. The first one assumes a stationary state and fits a single transfer function based on an exponential integral equation, of the form $\tilde{g}_0(x_1, x_2, t) = x_1 \int_{x_2} \frac{e^{-t}}{t} dt$ with x_1 and x_2 being the optimization parameters, to the experimental temperature: $\hat{g}_0(t_i) = \min_{x_1, x_2} \left\| \left(f(t) * \tilde{g}_0(x_1, x_2, t) \right) - T_{Exp}(t) \right\|_2$. The temperatures with this method are not well reproduced in a non-stationary scenario, since only one set of circulating flow and bleed rates (i.e., state) is considered. To enhance the fit, one transfer function per state $\hat{g}_s$ can be obtained by scaling the initial function $\hat{g}_0$ by coefficients a_s, i.e., $\hat{g}_s(t) = a_s \cdot \hat{g}_0(t)$. The coefficients a_s are obtained through the minimization with non-stationary convolution:

$a_s = \min_{a_s} \left\| \left(f * (a(s) \cdot \hat{g}_0)\right)(t) - T_{Exp}(t) \right\|_2$. The main optimization will then use the set of $\hat{g}_s(\tau_j)$ evaluated at nodes τ_j for each state s as the initial solution.

VALIDATION SCENARIOS

To assess the performance of the proposed deconvolution algorithm and to fulfill the objective of the paper, two test cases are used. The first one is a set of four year-long numerical simulations with different sets of constant operating parameters of a GSHP system using a SCW. This case will be used to obtain long-term transfer functions with the stationary deconvolution. The second case is a field TRT of 30 days with time-varying circulating flow and bleed rates. This case will employ the deconvolution to retrieve an experimental set of transfer functions with the non-stationary deconvolution.

The stationary case is made using the numerical model based on the work of Beaudry et al., (2022) on a system with 5 SCWs. The recordings have time steps of one hour, over a year of operation. Four simulations were generated, each using different constant sets of operating circulating flow and bleed rates, as described in Table 1. Each state is described by its respective numerically generated transfer function. Then, temperatures T_{out} are generated by applying a superposition principle (or convolution) to the known ground heating power profile and the numerical transfer functions. These signals are then used in a stationary deconvolution to obtain the long-term transfer function.

The non-stationary case has samplings at every minute and is performed on the SCW site described by Beaudry et al. (2018, 2019), which was built in Varennes, Quebec. The SCW is 215 m deep and an injection well of 150m was dug at about 10 m from the main well to receive the bled flow rate. The TRT was performed in July 2019 and varies the heating power, the circulating and bleed rates to stimulate the well under non-stationary operating conditions. In total, 4 successive states occur during the TRT and are described in Table 1. Two different circulating flow rates are used, and a bleed flow rate of approximately 10% is activated in the middle of each sequence. To minimize the impact of high frequency noise on the data, a moving average filter with a window of 10 points was used on both the temperature and heating power of the field TRT. For both test cases, the physical parameters are reported in Table 2.

Table 1. Circulating flow and bleed rates for the four different states used for the stationary and non-stationary cases.

Test case	Flow rate	g_1	g_2	g_3	g_4
Stationary	Circulating (L/min)	326	408	489	568
	Bleed (L/min)	65	82	98	170
Non-stationary	Circulating (L/min)	71	71	145	145
	Bleed (L/min)	0	7	0	15

Table 2. Thermal properties of the numerical model used for the stationary (left) and non-stationary (right) cases.

Parameter	Symbol	Unit	Ground	Pipe	Water
Volumetric Heat Capacity	ρCp	kJ m^{-3} K^{-1}	2160 | 2070	2000 | 2174	4187 | 4176
Porosity	n	-	0.01 | 0.02	0 | 1e-05	1 | 1
Thermal Conductivity	k	W m^{-1} K^{-1}	3.99 | 2.78	0.45 | 0.42	0.57 | 0.59
Hydraulic Conductivity	K	m s^{-1}	6.5e-5 | 5.7e-7	1e-9 | 1e-09	1000 | 1000
Specific storage	S_s	m^{-1}	1e-4 | 6.4e-4	4e-6 | 4e-10	4e-6 | 4e-10

RESULTS

Stationary case – Simulated temperatures

In Figure 1, the results of the stationary deconvolution applied to four different simulations are presented. It can be noted that both the transfer functions and the temperature are reproduced with great accuracy. The RMSE of the various transfer functions are all less than 0.001 °C/W and the RMSE of the 4 temperature fits are of less than 0.044 °C. In all cases, the constraints C_1 and C_2 are always respected. Indeed, each case shows strictly growing transfer functions and strictly downward first derivative slope from the beginning of the transfer functions, showing that the value z in the constraint C_2 can be taken as the first hour of operation. The larger deviations on the curves are at the end of the functions and mostly visible on the derivatives. All the stationary deconvolution converged in under 30 seconds.

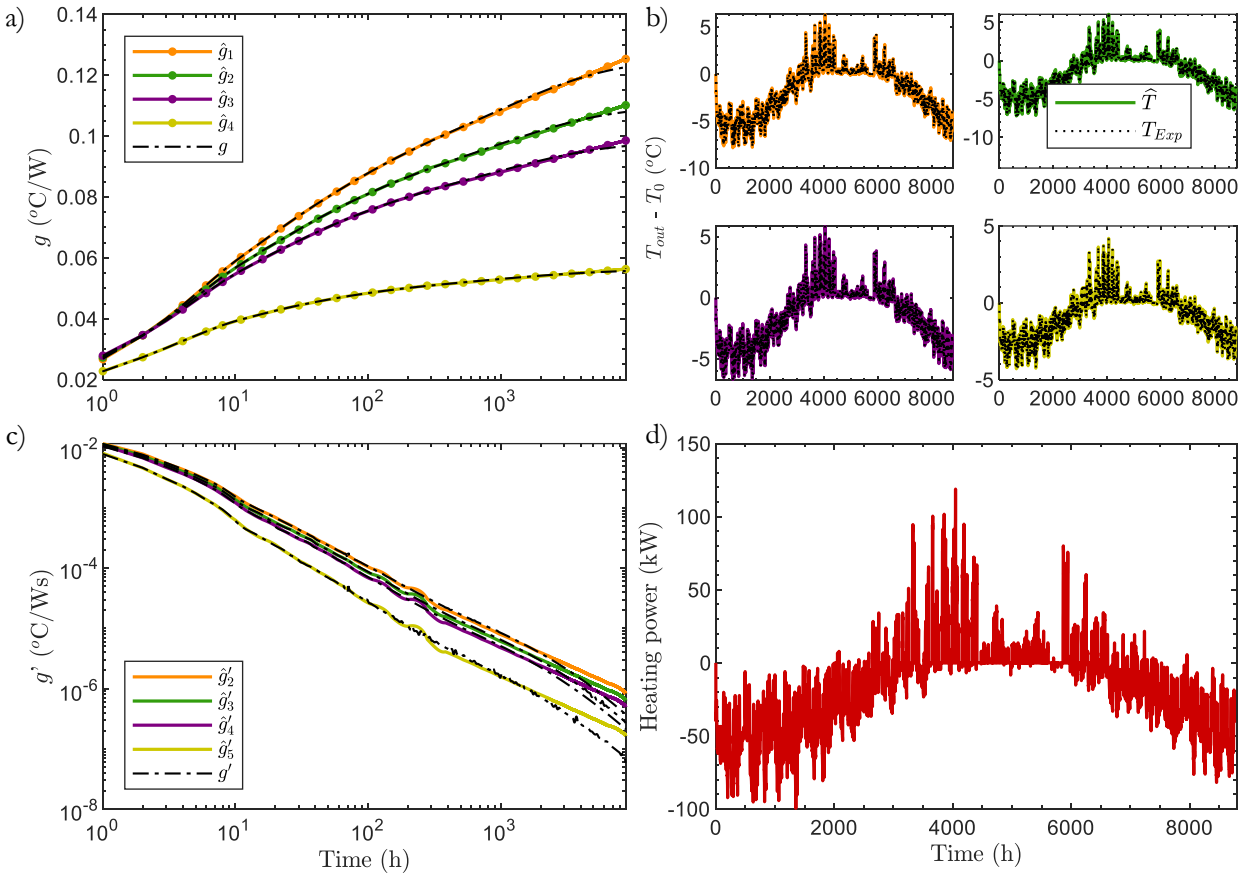

Figure 1. Stationary deconvolution results on 4 numerical test cases using the same heating power profile. a) and c) Deconvolved and numerical transfer functions and their derivatives respectively. b) Convolved and simulated temperatures. d) Heating power profile used in each deconvolution. The dots in a) show the nodes τ_j. The RMSE for the 4 cases are respectively: 0.04, 0.04, 0.03 and 0.01 °C.

Non-Stationary Case – Experimental Temperatures

In Figure 2, the results of the non-stationary deconvolution applied to the TRT experimental data are shown, with the associated temperature RMSE being of 0.19 °C. One can notice that the transfer functions are not all the same length. Instead, they are only illustrated on their respective activation time. This means that, for example, the function corresponding to the first state (i.e., flow rate of 71 L/min and bleed rate of 0 L/min) is only used for the first 8 days of the TRT. The second function, corresponding to the second state (i.e., flow rate of 71 L/min and bleed rate of 7 L/min), is used on the first 16 days since the first 8 days impact the temperature between 8 and 16 days. The vertical lines on Figure 2 shows the ending moment of each transfer function.

The algorithm converged in only 57 iterations and 35 minutes but had difficulty to enforce the C_2 constraint, as can be seen in Figure 2 c). This could be explained by the difficulty of the algorithm to find a global minimum due to the large number of nodes to optimize. Indeed, each function has 22 nodes, which amount to 88 parameters to estimate on a test composed of 43200 data points.

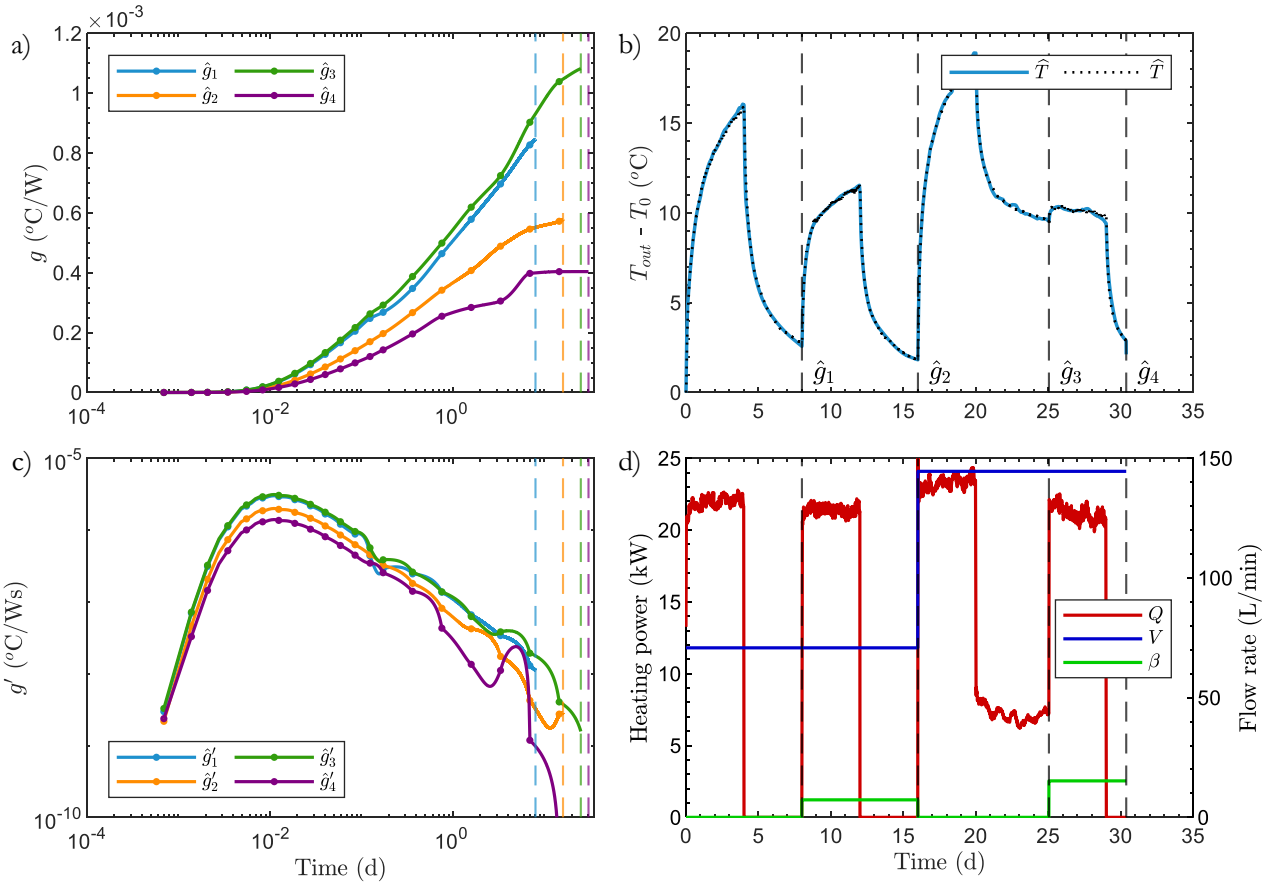

Figure 2. Non-stationary deconvolution result on an experimental TRT with 4 successive states. a) and c) Length dependent deconvolved transfer functions and their derivatives respectively. b) Convolved and experimental temperatures. d) Heating power (Q) profile, circulating flow (V) and bleed (β) rates used in each deconvolution. The dots on the curves in a) show the location of the nodes τ_j. The temperature RMSE is 0.19 °C.

DISCUSSION

The results show that both the stationary and non-stationary deconvolution algorithms are quite good at reproducing the temperature of either the year-long simulation or the long field TRT. This stems from the use of the temperature as the sole factor in the objective function of Eq. 2. In the stationary deconvolution algorithm, the transfer functions show a great fit with the numerical ones. Although the experimental ones are not available for the TRT, the transfer functions are not as smooth as expected. This could stem from the way the optimization problem is set to optimize only the temperature fit. Note, however, that the fluctuations of the first derivative appear visually exaggerated using a log-log scale. One way to smooth the transfer function could be to add regularization terms to the objective function.

Also, it is noticeable that the constraint C_2 described at Eq. 4 is not always respected during the non-stationary deconvolution. This is apparent by the slope of the transfer function first derivatives that are not always negative after around 3 hours of test. This last value was taken arbitrarily, to ensure that the TRT was in a relative steady state. In that section of the transfer function, the first derivative's slope should be strictly downward, as can be seen in the stationary deconvolution in Figure 1. In Figure 2, some functions show positive first derivative at long times, even if the nodes show a downward trend for these times. Indeed, PCHIP interpolation ensures that g is increasing but not that its derivative behaves as desired. This shows the complexity of the inversion problem, and that further work is needed to obtain in non-stationary case transfer functions with all the desired properties.

It is worth noting that for both stationary and non-stationary deconvolution, the measurement errors of the flow and bleeding flow rates are simplified to continuous or step signals. The flow rates shown in Figure 2 are segmented averages of their measured signals. However, these signals are affected by natural variation and measurement errors. This simplification is used to ensure that a limited number of transfer functions are deconvolved. Otherwise, there could be as much transfer functions as data point in the flow rates signals. The impacts of such a simplification are hard to estimate but are to be considered when analyzing deconvolution results.

Finally, an aspect limiting the fit in the non-stationary case is the precision of the forward model. In Beaudry et al.(2021), it is mentioned that the non-stationary convolution method has higher residuals within the fluid residence time due to slight imprecision in the correction function. Also, vertical temperature profiles are not considered in the current application of the forward model. This could represent an additional error since it was demonstrated that it has a significant influence on the groundwater temperature along the borehole wall in SCW operations (Beaudry et al., 2019).

CONCLUSION

In this article, a deconvolution algorithm was used both in stationary and non-stationary conditions to recover transfer functions related to the operating parameters occurring in the GHE. The stationary deconvolution showed that long-term transfer functions can be obtained, and the application of non-stationary deconvolution was demonstrated on an experimental test case. It has been shown that the experimental temperature can be recovered with temperature fits with accuracies of less than 0.05 °C with stationary deconvolution and 0.2 °C with non-stationary deconvolution.

This algorithm has the potential to help GHE response simulation by providing a way to obtain experimental transfer functions on both stationary and non-stationary scenarios. The extension of the deconvolution toward non-stationary situations makes the algorithm more flexible and applicable to a larger set of situations that can be encountered in field application, such as GSHP systems that have been operating for several years or with time-varying flow rates. In this case, the deconvolution can be applied to validate the performance of the system.

ACKNOWLEDGMENTS

The authors wish to acknowledge the support and funding provided by the Natural Sciences and Engineering Research Council of Canada (grant number RDCPJ 530945), the Trottier Energy Institute, Hydro-Québec, FTE drilling, Marmott Energies, Richelieu Hydrogeology and Versaprofiles.

NOMENCLATURE

a = Scalar weights to roughly adjust $\hat{g}_{0,Set}$ (-)
β = Bleed flow rate (L/min)
C = Constraint applied on the nodes in the optimization problem (-)
E = Objective function to evaluate (-)
f = Incremental heating power function (W)
g = Transfer function (°C/W)
τ = Nodes used as optimization parameters (-)
Q = Heating power (W)
T = Temperature (°C)
V = Circulating flow rate (L/min)

Subscripts

Exp = Experimental
0 = Initial
out = Borehole outlet
s = State identifier
Set = Group of transfer functions

REFERENCES

Beaudry, G., Pasquier, P., & Marcotte, D. (2018). Hydrogeothermal characterization and modelling of a standing column well experimental installation. *Proceedings of the IGSHPA Research Track 2018*, 1–10. https://doi.org/10.22488/okstate.18.000009

Beaudry, G., Pasquier, P., & Marcotte, D. (2019). The impact of rock fracturing and pump intake location on the thermal recovery of a standing column well: Model development, experimental validation, and numerical analysis. *Science and Technology for the Built Environment*, *25*(8), 1052–1068. https://doi.org/10.1080/23744731.2019.1648133

Beaudry, G., Pasquier, P., & Marcotte, D. (2021). A fast convolution-based method to simulate time-varying flow rates in closed-loop and standing column well ground heat exchangers. *Renewable Energy*. https://doi.org/10.1016/j.renene.2021.04.045

Beaudry, G., Pasquier, P., Marcotte, D., & Zarrella, A. (2022). Flow rate control in standing column wells: A flexible solution for reducing the energy use and peak power demand of the built environment. *Applied Energy*, *313*, 118774. https://doi.org/10.1016/j.apenergy.2022.118774

Beier, R. A. (2020). Deconvolution and convolution methods for thermal response tests on borehole heat exchangers. *Geothermics*, *86*, 101786. https://doi.org/10.1016/j.geothermics.2019.101786

Cimmino, M., & Bernier, M. (2013). Preprocessor for the generation of g-functions used in the simulation of geothermal systems. *BS2013*, 8.

Dion, G., Pasquier, P., & Marcotte, D. (2022). Deconvolution of experimental thermal response test data to recover short-term g-function. *Geothermics*, *100*, 102302. https://doi.org/10.1016/j.geothermics.2021.102302

Dusseault, B., Pasquier, P., & Marcotte, D. (2018). A block matrix formulation for efficient g-function construction. *Renewable Energy*, *121*, 249–260. https://doi.org/10.1016/j.renene.2017.12.092

Eskilson, P. (1987). *Thermal Analysis of Heat Extraction Boreholes*. 222.

Marcotte, D., & Pasquier, P. (2014). Unit-response function for ground heat exchanger with parallel, series or mixed borehole arrangement. *Renewable Energy*, *68*, 14–24. https://doi.org/10.1016/j.renene.2014.01.023

Nguyen, A., & Pasquier, P. (2021). A successive flux estimation method for rapid g-function construction of small to large-scale ground heat exchanger. *Renewable Energy*, *165*, 359–368. https://doi.org/10.1016/j.renene.2020.10.074

Robert, F., & Gosselin, L. (2014). New methodology to design ground coupled heat pump systems based on total cost minimization. *Applied Thermal Engineering*, *62*(2), 481–491. https://doi.org/10.1016/j.applthermaleng.2013.08.003

Wei, J., Wang, L., Jia, L., & Cai, W. (2016). A new method for calculation of short time-step g-functions of vertical ground heat exchangers. *Applied Thermal Engineering*, *99*, 776–783. https://doi.org/10.1016/j.applthermaleng.2016.01.105

Zanchini, E., & Lazzari, S. (2014). New g-functions for the hourly simulation of double U-tube borehole heat exchanger fields. *Energy*, *70*, 444–455. https://doi.org/10.1016/j.energy.2014.04.022